

# An Optical Tool-Setting Scheme for Ultra Precision Machining

Tai-An Cheng<sup>\*</sup>, Choung-Lii Chao<sup>\*\*</sup>, Der-Chyuan Lou<sup>\*</sup>, and Chung-Woei Chao<sup>\*\*\*</sup>

<sup>\*</sup> Department of Electrical Engineering, Chung Cheng Institute of Technology, National Defense University

<sup>\*\*</sup> Department of Mechanical and Electro-Mechanical Engineering, Tam-Kang University,

<sup>\*\*\*</sup> Department of Information Management, Hsing-Wu College

## ABSTRACT

Tool setting is one of the key procedures in ultra-precision diamond turning operation. The conventional tool setting procedure using a touch-probe is time-consuming, laborious and running a great risk of damaging the delicate tool-tip. The optical/non-contact way of tool setting has the advantage of not having to touch the tool, but its resolution is limited by the optical diffraction limit and the resolution of the CCD (charge coupled device). A new optical tool setting scheme with submicron accuracy is presented in this paper and the results demonstrated good efficiency and higher accuracy in comparison to the other tool setting techniques.

**Keywords:** tool-setting, ultra-precision machining, sub-pixel

## 光學刀具定位系統於超精密加工之應用

鄭泰安<sup>\*</sup> 趙崇禮<sup>\*\*</sup> 婁德權<sup>\*</sup> 趙崇偉<sup>\*\*\*</sup>

<sup>\*</sup>國防大學中正理工學院電機系 <sup>\*\*</sup>淡江大學機電系 <sup>\*\*\*</sup>醒吾技術學院資管系

## 摘要

刀具定位係超精密切削加工作業中重要且必需的步驟，傳統上探針式定位方法往往為耗時費力的程序，而光學式定位方法具安全且非接觸之優點，惟通常受限於光線繞射影響與電子攝影機解析度限制，在本文中發展一個次微米之光學式刀具定位方法，由實驗結果驗證本方法效能遠較傳統定位方法高。

**關鍵詞：**刀具定位，超精密加工，次像素

## I. INTRODUCTION

Tool setting is to align the tool tip with the rotation axis of spindle and is the first thing to be done before the turning process can actually start. Misaligning the tool will introduce form error of the generated parts and may cause undesired damage to the cutting tool. Therefore, an effective and precise tool setting technique is of essential importance in ultra-precision machining operation.

There are already many methods such as probing, laser proximity sensing technique and optical inspection etc., developed and tried for tool setting [1, 2]. However, most of these schemes are not easy to be adapted for practical in-situ application. The major problem for touch-probe setting technique is running the risk of damaging the diamond tool and its resolution depends on the positioning accuracy of the stylus (1~10 $\mu$ m). Vision-based techniques, on the other hand, have the advantages of doing the measurement non contact and in-process [3, 4]. However, its accuracy is limited by the resolution of the image system ( $\mu$ m/pixel) which cannot meet the requirement of precision diamond turning operation. The typical resolution of an ultra-precision turning machine (1~10nm) at the present time is almost one thousandth the resolution of typical image system ( $\mu$ m/pixel).

Many researches applying optical/non-contact techniques have been conducted to improve the tool setting system in recent years [5, 6]. Chao et al. [7] proposed a scheme of using edge-detection image processing and sub-pixel dividing techniques in conjunction with the CNC (computer numerical control) controller of precision turning machine to improve the tool setting accuracy. This scheme required many fine movements to provide data for statistically averaging out the measurement error. However, the large amount of tool images, typically 100~500 frames, needed to determine a tool tip position at submicron precision has hindered its industrial application. Therefore, not only accuracy but also efficiency has to be taken into account if the tool setting scheme is to be used in industry.

In the present study, a new tool setting scheme based on Zernike moments operator and curve fitting technique is proposed and tested. The

Zernike moment is used in the scheme to refine the tool-tip from the image frames and the curve fitting technique is to minimize the influence of noise and determine the tool-tip with submicron accuracy.

## II. TOOL TIP LOCALIZATION ANALYSIS TECHNIQUES

The proposed optical setting system has three major processing steps to go through: 1. Based on the captured image frames, a series of edge images (edge maps) are obtained by employing Canny operators, 2. Extracting tool tip from edge maps to produce a set of tip points and a two-order Zernike operator is then used to refine the tip position with submicron accuracy, 3. Curve fitting is adopted to minimize the influence of step fluctuation and to compute the precise tip position. The schematic diagram of the proposed tool setting system is shown in Fig. 1.

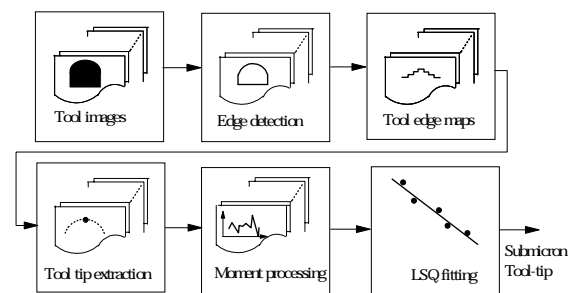


Fig.1. Schematic diagrams of proposed scheme.

### 2.1 Tool edge extraction using Canny operator [8]

The Canny operator is an efficient edge detector that had been used extensively in computer vision applications. Adopting a multi-step edge detection procedure, the Canny operator enables to find the optimal object boundaries in pixel-level precision.

The Canny edge detection can be summarized as: (1) smoothing step: smooth the image with a Gaussian convolution to reduce image details and noises, (2) enhancement step: compute gradient magnitude and gradient direction at each pixel, (3) localization step: identify edge points by non-maximal suppression

to find the local maxima in the direction of the gradient, (4) labeling step: eliminate insignificant edges by hysteresis threshold to reduce the false edge and ensure a real edge will not be split into several small segments.

## 2.2 Zernike moments [9-11]

Zernike moments define a set of orthogonal polynomials over the interior of the unit circle. For digital image processing, the Zernike moments  $Z_{nc}$  of order  $n$  with repetition  $c$  of image intensity functions  $f(x, y)$  can be written in the XY-plane:

$$Z_{nc} = \frac{n+1}{\pi} \sum_x \sum_y f(x, y) R_{nc}(x, y) \quad (1)$$

The Cartesian radial polynomial is written as:

$$R_{nc}(x, y) = \sum_{k=0}^{(n-|c|/2)} \frac{(-1)^k (n-k)!}{k!((n+|c|)/2-k)!((n-|c|)/2-k)!} (x^2 + y^2)^{n-2k} \quad (2)$$

where  $n$  is an integer and  $n - |c|$  is even.

The edge parameter  $L$  is that the distance from the center of the circular kernel to determine edge points can be expressed as:

$$L = \frac{Z_{20}}{Z'_{11}} \quad (3)$$

where  $Z'_{11}$  is the imaginary component of first-order moments and  $Z_{20}$  is the real component of second-order moments.

## III. THE PROPOSED TOOL SETTING SCHEME

The proposed scheme was motivated from how to couple image processing with precision positioning stage. The setting procedures can be summarized as follows:

Step1. Move the nano-positioning stage and capture tool images for all the specified movement.

Step2. Utilize Canny edge detector to extract edge map from image frames.

Step3. Locate tool tips from edge maps.

Step4. Apply the Zernike moments to figure out the tool tips position.

Step5. Refine the precision tool tip position using curve fitting technique.

## 3.1 Tool-tip localization and pixel step fluctuation

Those images of tool captured by CCD/frame grabber were stored in a computer for further processing. The sequence of tool images can be expressed as:

$$f_n(x, y) = f(x(t_n), y(t_n), t_n) \quad (4)$$

where the functional  $f_n(x, y) = f(x(t_n), y(t_n), t_n)$  is the  $n$ th sampled image captured at step  $t$  of stage movement. All acquired images were then processed with Canny operator to locate the profile in camera coordinates (pixel locations). The tool edge detection by Canny operator can be represented as:

$$E_n(x, y) = C[f_n(x, y), T, \sigma] \quad (5)$$

where  $T$  is the upper threshold and  $\sigma$  is the Gaussian parameter for Canny edge detection. In this study, the value  $\sigma$  is 1.0 and the lower threshold for finer edges used is  $0.4T$ . After the tool edge maps have been extracted, the key issue followed was to decide the tip position. Depending on which way the stage is moving, the tool tip can be defined as the top-most pixel which has the maximum or minimum value of the Y axis. The sequence of tip points  $TP_n(x, y)$  produced from tool images are shown in Fig.2 and calculated by:

$$TP_n(x, y) = Top(E_n(x, y)) \quad (6)$$

## 3.2 Precision improvement using Zernike moments

To further improve the setting precision, a moment-based operator was then used to

determine the location of tip point. In this study, the Zernike convolution mask is designed to be 7 by 7. Generally speaking, using a larger mask size has the advantage of reducing noise. However, this will increase the computational load.

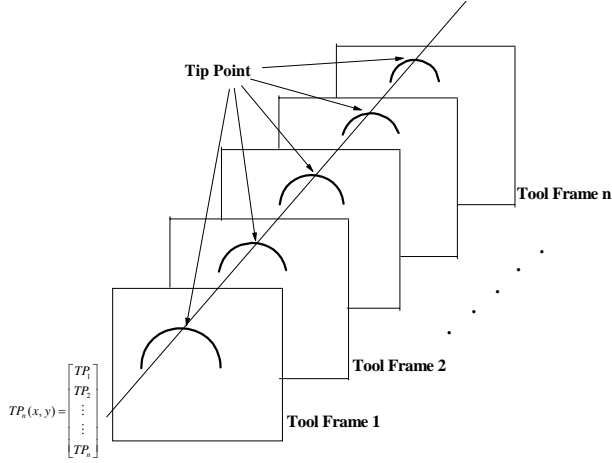


Fig.2. Tool tip detection results representation from a tool image sequence.

Masks of  $Z_{11}$  (the real component),  $Z'_{11}$  (the imaginary component) and  $Z_{20}$  were designed based on method suggested by Qu et al. [10]. For each tip point  $TP_n(x, y)$ , place Zernike masks to center at the tip point and compute the Zernike moments. According to Eq.3, tip point with sub-pixel accuracy is determined by:

$$TP_{Zernike,n} = TP_n \left( \frac{Z_{20}}{Z_{11}} \right) \quad (7)$$

### 3.3 Refine the tip position from step fluctuation

The precision of an ultra-precision diamond turning machine, at present time, is normally in the order of 1~10nm. The resolution of a CCD optical measuring system, is typically around 1~10 $\mu$ m. Owing to the large discrepancy between the digital image system and the precision positioning stage, the digital image system is relatively insensitive to stage steps and can only respond when the movement has built up and reached a critical value. This means that there is a step-like displacement shown by the pixels over the stage step.

The pixel step is greatly influenced by fluctuation due to the noise introduced by the optical effects such as lighting system, vibration and diffraction etc. These effects are usually worsened when approaching each switching point where tool tip is moving across to another pixel. Fig.3 is the fluctuation of tool-tip movement shown by the pixels. Because of CCD sampling, the detected tip positions appeared to be a combination of small pieces of line segments.

Using this approach, the Zernike moment process cannot converge correctly when approaching each switching point where tool tip is moving across to another pixel. For this reason, curve fitting technique is applied to reduce the noise and to increase the setting precision.

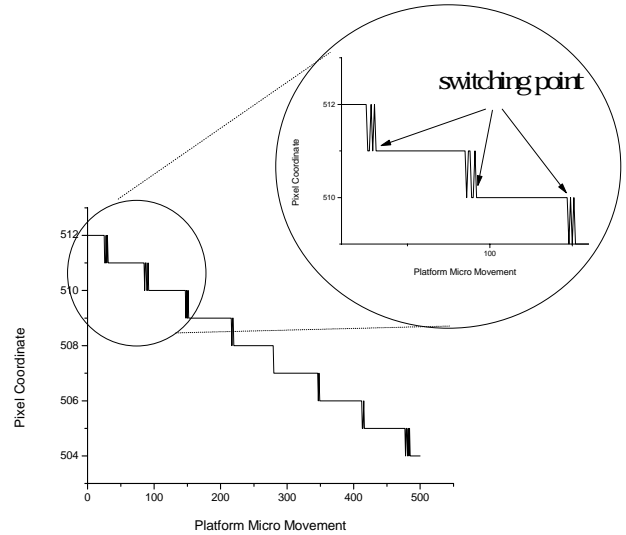


Fig.3. Fluctuation of the tool-edge movement shown by the pixels.

The method uses an equation  $y = f(x) = ax + b$  that has the minimal sum of the deviations squared error from a given tip point data set  $(x_1, y_1), (x_2, y_2), \dots, (x_n, y_n)$ . A 2D line fitting models namely least squares method is used for approximating the tool tip points. The curve fitting process is expressed as followed:

$$(\hat{x}, \hat{y}) = \left\{ (x_i, y_i) \mid \min \left( \sum_{i=1}^n (y(i) - f(x_i))^2 \right) \right\} \quad (8)$$

and

$$|x_n - x_1| = d \quad (9)$$

where  $d$  is a specified assessment distance and  $x_1, x_n$  is the starting and ending point, respectively. The position of the tool tip point is then obtained by locating the center point of the fitting line and is expressed as:

$$TP_{measured}(x_m, y_m) = Mid(\hat{x}, \hat{y}) \quad (10)$$

## IV. EXPERIMENTAL SET-UP AND TOOL FRAME ACQUISITION

Experiments are conducted to validate the performance of the proposed tool setting scheme and the obtained results are compared to other schemes. The details of the experimental procedures for tool setting using the proposed scheme are described in the following sections.

### 4.1 Experimental setup

A positioning stage of 100nm positioning resolution is used for the setting tests. The diamond tool is held by a tool post on the stage, calibrated by an interferometer (10nm resolution). The stage itself is standing on an air bearing slide, driven by linear motor. To further minimize the vibration, all the system mentioned above are placed on an air-suspension table for vibration isolation. All devices and processes, including the fine movements of stage/tool, are controlled by a PC. A CCD is equipped above the tool post to measure tool geometry.

Image frames captured by CCD after each fine movements were transmitted to the image processing units. The pixel size used in the test was  $6.39\mu\text{m}$  for sharp tool and  $2.58\mu\text{m}$  for round tool. The schematic of experimental setup is shown in Fig.4.

### 4.2 Tool frame acquisition

Two types of diamond tools (sharp tool and round tool), having different geometry and cutting edges, were used in the tool setting experiments to check the accuracy and the efficiency of the proposed scheme. The profile of the tools used in

the present study were examined using SEM (shown in Fig.5(a),(b)). The increase in chamber pressure resulted in, as shown in Fig.5, a decrease in corresponding etch rate. It was also found in this study that, having all etching parameters fixed, the etch rate got lower with time (as shown in Fig.6).

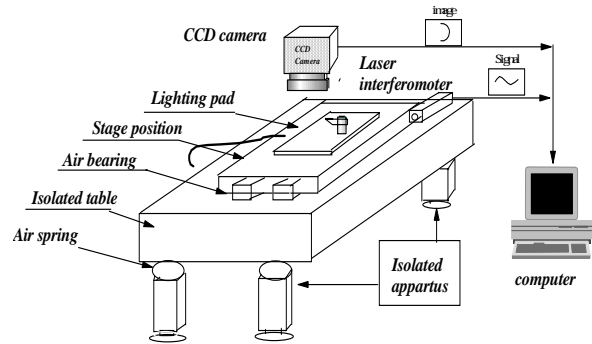


Fig.4. The experimental apparatus in this study.

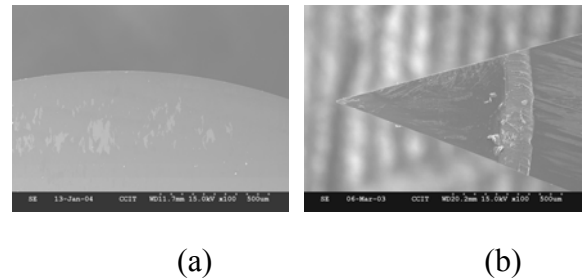


Fig.5. SEM micrographs of two types of a diamond tools used in this study (a) round tool, (b) sharp tool.

The positioning stage was driven to move along the slide direction and in a step-by-step (the sampling interval) manner. The tool images were captured by CCD/frame-grabber for each and every steps along the way. A total of 5 different total assessment distances ( $10\mu\text{m}$ ,  $20\mu\text{m}$ ,  $30\mu\text{m}$ ,  $40\mu\text{m}$  and  $50\mu\text{m}$ ) and 4 sampling intervals ( $0.1\mu\text{m}$ ,  $0.2\mu\text{m}$ ,  $0.4\mu\text{m}$  and  $0.8\mu\text{m}$ ) were used for each diamond tool, resulting in 4 sequences of images. Consequently, all frames were processed by proposed image scheme to determine the tool tip position.

## V. RESULTS AND DISCUSSION

### 5.1 Setting accuracy and assessment distance

In practical, the number of tool frame depends on the assessment distance because tool image is captured for every fine movement within the assessment distance. Several schemes namely Chao's scheme, direct mean scheme, moment without least square scheme and proposed scheme were tested in this study for comparison purpose. Five different assessment distances (10~50 $\mu\text{m}$ ) were selected to evaluate all above mentioned schemes to check the influence of assessment distance on the achievable accuracy.

Shown in Fig.6 and Fig.7 are the results of setting accuracy obtained by various setting schemes plotted against assessment distances using a sharp and round tool respectively. It is easily seen that direct mean scheme ( $\blacktriangle$ ) and moment without least square scheme ( $\blacktriangledown$ ) have their limits in achievable accuracy around 1.2 $\mu\text{m}$  and 0.4 $\mu\text{m}$  respectively. As to the Chao's scheme ( $\blacksquare$ ), it normally takes 30 to 40 $\mu\text{m}$  assessment distance to get the setting accuracy within 0.2 $\mu\text{m}$  margin which is required for precision diamond turning. The proposed scheme ( $\bullet$ ) performed rather well in having the setting accuracy around 0.2 $\mu\text{m}$  in a very short of assessment distance (10 to 20 $\mu\text{m}$ ).

The setting accuracies obtained from direct mean scheme and moment without least square scheme is relatively low that can be attributed to the impact of noise disturbances and many detailed tip information in the tool images is lost. The results from setting both tools have suggested that the proposed scheme offered a better performance than the other schemes.

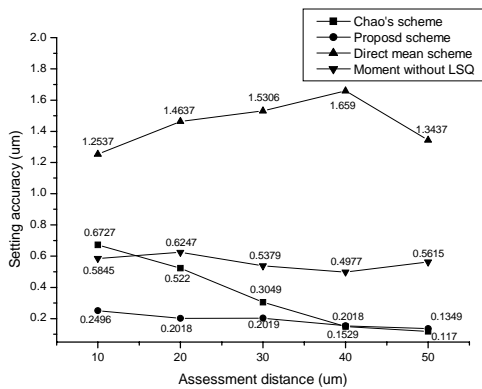


Fig.6. Comparison of the positioning accuracy of Chao's, direct mean, moment without LSQ and proposed scheme. (sharp tool, frame number : 500)

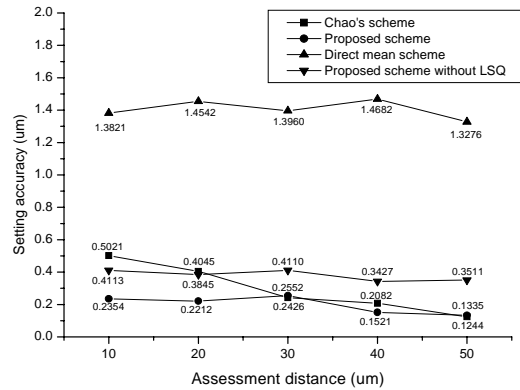


Fig.7. Comparison of the positioning accuracy of Chao's, direct mean, moment without LSQ and proposed scheme. (round tool, frame number:500)

## 5.2 Frame number and setting accuracy

Apart from good accuracy, efficiency, that is the time required to achieve the targeted result, is another important requirement for industrial application. Generally, the more image frames needed the longer it takes to finish. Shown in Fig.8 and Fig.9 are the results of setting accuracy obtained by various setting schemes plotted against number of frames using a sharp and round tool respectively.

The general trend for all the schemes investigated was that the larger the number of frames the better the setting accuracy. Amongst these schemes investigated, direct mean scheme and moment without least square scheme still could not make the setting accuracy reached the 0.2 $\mu\text{m}$  target. Chao's scheme could achieve setting accuracy of 0.2 $\mu\text{m}$  only when the number of frames reached about 250 while the proposed scheme needed only 10 to 100 frames. The setting accuracy is enhanced due to the increase of frame number in the assessment distance.

It is worth noting also that Chao's scheme can further improve the setting accuracy by increasing the number of frames but the proposed scheme can not get too much by increasing number of frames (the setting accuracy remains around 0.2~0.25 $\mu\text{m}$ ). However, given the setting accuracy of 0.2~0.25 $\mu\text{m}$ , the proposed technique is much faster than that of Chao's scheme using only a fraction of the frames required by Chao's scheme.

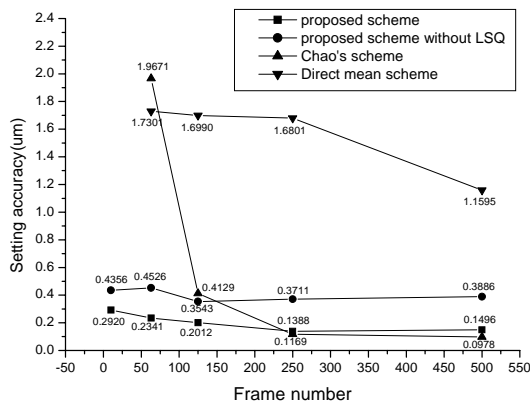


Fig.8. Frame needed of Chao's, direct mean and proposed scheme. (sharp tool)

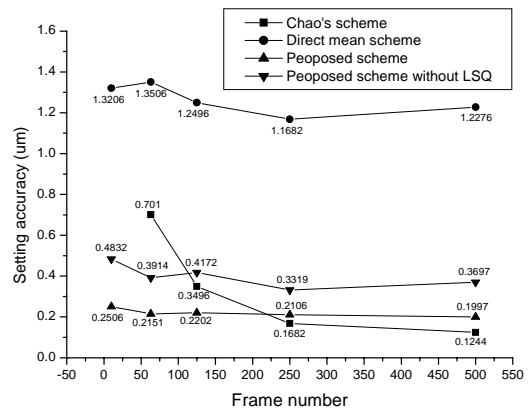


Fig.10. Comparison of setting accuracy between round tool and sharp tool. (frame number:250)

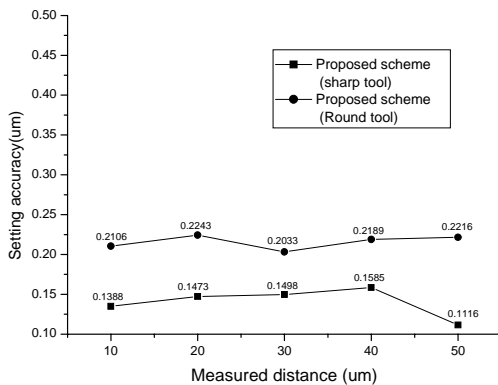


Fig.9. Frame needed of Chao's, direct mean and proposed scheme. (round tool)

### 5.3 Influence of tool geometry

Tool of all kind of shapes and sizes can be used in diamond turning. Two most commonly used tool shapes are sharp tool and round nose tool. Shown in Fig.10 is the setting accuracy obtained by detecting the tool tips of the round nose tool and sharp tool using the proposed scheme.

There is an overall accuracy average of  $0.13\mu\text{m}$  for sharp tool and  $0.26\mu\text{m}$  for round tool as showed in Fig.8. It can be seen the sharp tool sustained less setting error than round tool and can be attributed directly to the edge geometry characteristics.

## VI. CONCLUSIONS

A new optical tool setting scheme has been developed and implemented in this study. The proposed scheme together with several other non-contact tool setting schemes were adopted to set the two most commonly used diamond tools namely sharp tool and round tool in position. The results showed that, in comparison to the other tool setting techniques, the proposed scheme demonstrated better efficiency and good accuracy. The experimental results have verified that the setting accuracy of the proposed scheme was around  $0.2\mu\text{m}$  which was very close to Chao's scheme but the frame needed was greatly reduced (nearly 50 times). This indicates that the proposed scheme is much more efficient and more suitable for fast and accurate tool setting.

## REFERENCES

- [1] Soãres, S., "Nanometer Edge and Surface Imaging Using Optical Scatter," Precision Engineering, Vol. 27, pp. 99-102, 2003.
- [2] Hyong, T. K., Chang, S. S., and Hae, J. Y., "Two-Step Algorithm for Automatic Alignment in Wafer Dicing Process," Microelectronics Reliability, Vol.44, pp. 1165-1179, 2004.
- [3] Jurkovic, J., Korosec, M., and Kopac, J., "New Approach in Tool Wear Measuring Technique Using CCD Vision System," Journal of Machine Tools and Manufacture,

- Vol. 45, pp. 1023-1030, 2005.
- [4] Wang, W. H., Hong, G. S., and Wong, Y. S., "Flank Wear Measurement by a Threshold Independent Method With Sub-Pixel Accuracy," *Journal of Machine Tools and Manufacture*, Vol. 46, pp. 199-207, 2006.
  - [5] Lahajnar, F., Bernard, R., Pernuš, F., and Kovačič, S., "Machine Vision System for Inspecting Electric Plates," *Computer in Industry*, Vol. 47, pp. 113-122, 2002.
  - [6] Zhou, M., and Ngoi, B. K. A., "Factors Affecting Form Accuracy in Diamond Turning of Optical Components," *Journal of Materials Processing Technology*, Vol. 138, pp. 586-589, 2003.
  - [7] Chao, C. L., Cheng, T. A., Lou, D. C., and Chao, C. W., "Development of a Non-Contact Tool Setting System for Precision Diamond Turning," *Journal of Materials Science Forum*, Vol. 505-507, pp. 367-373, 2006.
  - [8] Canny, J., "A Computational Approach to Edge Detection," *IEEE Trans. on Pattern Analysis and Machine Intelligence*, PAMI-8, No. 6, pp. 679-698, 1986.
  - [9] Ghosal, S., and Mehrotra, R., "A Moment Based Unified Approach to Image Feature Detection," *IEEE Transactions on Image Processing*, Vol. 6, No. 6, pp. 781-793, 1997.
  - [10] Qu, Y. D., Cui, C. S., Chen, S. B., and Li, J. Q., "A Fast Sub-Pixel Edge Detection Scheme Using Sobel-Zernike Moments Operator," *Image and Vision Computing*, Vol. 23, pp. 11-17, 2005.
  - [11] Kamila, N. K., Mahapatra, S., and Nanda, S., "Invariance Image Analysis Using Modified Zernike Moments," *Pattern Recognition Letters*, Vol. 26, pp. 747-753, 2005.